scientific reports

Check for updates

OPEN

Effect of caffeine and other xanthines on liver sinusoidal endothelial cell ultrastructure

Hong Mao[1,2,8]✉, Karolina Szafranska[1,8]✉, Larissa Kruse[1], Christopher Holte[1], Deanna L. Wolfson[2], Balpreet Singh Ahluwalia[2], Cynthia B. Whitchurch[3], Louise Cole[3], Glen P. Lockwood[4,5], Robin Diekmann[6,7], David Le Couteur[4,5], Victoria C. Cogger[4,5] & Peter A. G. McCourt[1,4,5]

Xanthines such as caffeine and theobromine are among the most consumed psychoactive stimulants in the world, either as natural components of coffee, tea and chocolate, or as added ingredients. The present study assessed if xanthines affect liver sinusoidal endothelial cells (LSEC). Cultured primary rat LSEC were challenged with xanthines at concentrations typically obtained from normal consumption of xanthine-containing beverages, food or medicines; and at higher concentrations below the in vitro toxic limit. The fenestrated morphology of LSEC were examined with scanning electron and structured illumination microscopy. All xanthine challenges had no toxic effects on LSEC ultrastructure as judged by LSEC fenestration morphology, or function as determined by endocytosis studies. All xanthines in high concentrations (150 µg/mL) increased fenestration frequency but at physiologically relevant concentrations, only theobromine (8 µg/mL) showed an effect. LSEC porosity was influenced only by high caffeine doses which also shifted the fenestration distribution towards smaller pores. Moreover, a dose-dependent increase in fenestration number was observed after caffeine treatment. If these compounds induce similar changes in vivo, age-related reduction of LSEC porosity can be reversed by oral treatment with theobromine or with other xanthines using targeted delivery.

Coffee is one of the most widely consumed beverages meaning that any potential effects related to coffee intake will have significant global implications. Furthermore, most people drink coffee daily due to its stimulating effects. The main active ingredient in coffee—caffeine, can be found also in other beverages (tea, soft and energy drinks), food (guarana berries, chocolate), dietary supplements or even painkillers[1]. Formulations consisting of caffeine and either aspirin (a non-steroidal anti-inflammatory drug, NSAID) or paracetamol, are effective treatments for headaches[2] and sore throats[3] and caffeine has been shown to have an analgesic effect alone[4]. Many studies have investigated the associations between caffeine or coffee intake and health/diseases. Recently, the correlation between increased coffee consumption and improved neurocognitive functioning parameters was elicited in patients infected with human immunodeficiency virus (HIV) and hepatitis C virus (HCV)[5]. A different study showed that a sub-group of patients suffering from multiple sclerosis (MS) benefitted from additional coffee intake[6]. Interestingly, in a meta-analysis of studies about the effects of caffeine on Parkinson's disease (PD) caffeine appeared to both lower the rate of PD progression in patients suffering from the disease as well as decrease the risk of developing PD in the healthy population[7]. On the other hand, several studies have noted that an adjustment may be needed for an individual's caffeine dosage in relation to their age, sex and health conditions to maximize the positive and limit negative effects[8,9].

Caffeine is primarily metabolized in the liver to theobromine, theophylline and paraxanthine (Fig. 1). The demethylation process occurs in the hepatocytes via the cytochrome P450 enzyme system[10]. Overall, more

[1]Vascular Biology Research Group, Department of Medical Biology, Faculty of Health Sciences, University of Tromsø, The Arctic University of Norway, 9037 Tromsø, Norway. [2]Optical Nanoscopy Research Group, Department of Physics and Technology, Faculty of Science and Technology, University of Tromsø, The Arctic University of Norway, Tromsø, Norway. [3]Microbial Imaging Facility, The ithree Institute, University of Technology Sydney, Ultimo, NSW, Australia. [4]Centre for Education and Research, ANZAC Research Institute, Concord Repatriation General Hospital, Concord, NSW, Australia. [5]The Faculty of Medicine and Health, University of Sydney, Sydney, NSW, Australia. [6]Cell Biology and Biophysics Unit, European Molecular Biology Laboratory (EMBL), Heidelberg, Germany. [7]LaVision BioTec GmbH, Bielefeld, Germany. [8]These authors contributed equally: Hong Mao and Karolina Szafranska. ✉email: hong.mao@uit.no; karolina.szafranska@uit.no; szafranska.k.j@gmail.com

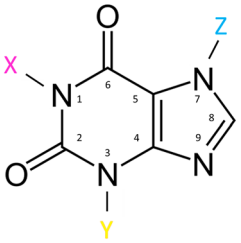

	X	Y	Z
Caffeine	CH_3	CH_3	CH_3
Theobromine	H	CH_3	CH_3
Theophylline	CH_3	CH_3	H
Paraxanthine	CH_3	H	CH_3

Figure 1. Chemical structure of xanthines. Caffeine (1,3,7-trimethylxanthine) is metabolized by demethylation in the liver to 3 main compounds: theobromine (3,7-dimethylxanthine), theophylline (1,3-dimethylxanthine) and paraxanthine (1,7-dimethylxanthine)[10].

than 25 metabolites have been identified in humans deriving from caffeine metabolism[11,12], with paraxanthine accounting for approximately 80% of the metabolites in the human liver[13,14]. In rats and mice, however, all three main metabolites of caffeine are present in similar amounts[15,16]. All the aforementioned primary metabolites are pharmacologically active and their plasma concentration may exceed that of caffeine in some stages due to their respective rate of metabolism and clearance[10], especially paraxanthine[16,17].

The liver, the body's largest internal organ, has the major role of detoxifying various metabolites in the human body. Liver sinusoidal endothelial cells (LSEC), which are located in hepatic sinusoids, play a fundamental role in maintaining the homeostasis and metabolic integrity of the liver[18]. LSEC are the most effective scavengers of blood-borne waste[19], regulate sinusoidal blood flow[20], trigger liver regeneration and contribute to hepatic complications, such as liver fibrosis and liver metastasis[18,21,22]. The distinct dynamic morphological features of LSEC—called fenestrations/fenestrae, enable bidirectional size-based transfer between the blood and the underlying hepatocytes. Fenestrations are non-diaphragmed nano-pores with diameters of 50–350 nm[23,24], and they are typically grouped in clusters called sieve plates[25,26]. The structural integrity of fenestrations is vital for the maintenance of regular exchange between the liver and the blood, and alterations in fenestrations can affect hepatocytes and liver function[26]. The regulation of fenestration size and frequency is not yet fully understood, but some signaling pathways have been shown to influence the formation of fenestrations[24]. For example, sildenafil (the active constituent of Viagra) was shown to improve porosity in both young and old mice[27], presumably via regulation of intracellular cGMP levels (via nitric oxide) and/or vascular endothelial growth factor (VEGF)-related/(VEGF)-independent pathways[28,29]. It should be noted however that other pathways may also be involved in the regulation of fenestration size and number (e.g., those mediated by calcium, regulated by myosin light chain (MLC)[24] or by alpha/beta-adrenergic receptors among others[30]).

Even though caffeine is primarily metabolized in hepatocytes, LSEC regulate transportation between the plasma and hepatocytes. Fenestrations create a dynamic barrier that can adapt to environmental conditions in a matter of seconds[31]. Caffeine intake is generally considered to be safe in moderate amounts (≤ 400 mg /day) in healthy adults[32,33], and with normal consumption the plasma concentrations are usually between 2–10 µg/mL (approximately 10–50 µM), rarely exceeding this[34]. Toxic effects occur for plasma concentrations of > 40 µg/mL[34,35]. The adverse effects of large doses of caffeine have been noted from early times, and these include nervousness, anxiety, insomnia, irregular heartbeats, excess stomach acid and heartburn[36]. However, it is important to understand that the liver can be exposed to far greater concentrations of caffeine and related compounds because the uptake takes place in the gastrointestinal (GI) tract. All the venous blood from the GI tract is collected into the portal vein, which then provides 75% of the blood inflow to the liver. This is the first-pass effect whereby the initial local concentration in the liver can be much higher while systemic plasma concentrations of the studied compound are lower[37].

Commercially available products rarely lead to toxic plasma concentrations of xanthines. A single standard cup of black coffee can yield a peak plasma caffeine concentration of about 2 µg/mL, while caffeine supplements can yield up to 10 µg/mL[38]. However, somewhat higher concentrations (8–20 µg/mL) are needed for the therapeutic effect of the caffeine metabolite theophylline in controlling asthma in adult humans[39,40]. Life-threatening effects were reported for the theophylline serum concentrations above 30 ug/mL[41]. Chocolate contains two methylated xanthine derivatives (caffeine and theobromine), which might potentiate their respective effects[42]. It was reported that 370 mg theobromine from chocolate (40-80 g of dark chocolate or 110 g of regular milk chocolate, roughly the size of a chocolate bar) was rapidly absorbed in humans and produces a plasma concentration of 8 µg/mL after 2 h[43–45]. In humans, paraxanthine plasma levels are usually higher than caffeine and can remain at a high level for a longer time due to the slower clearance and ongoing metabolism of caffeine[17].

Although coffee, chocolate, and other caffeinated substances such as tea are widely used all over the world, the effects of caffeine and its metabolites on LSEC have not been investigated. Here, we study the influence of xanthines on rat LSEC in both physiologically achievable concentrations as well as in higher concentrations that can simulate the first-pass effect.

Materials and methods

Rat LSEC production and cell culture. Sprague Dawley male rats (Animal Resource Centre, Murdoch, Western Australia; Charles River Laboratories, Sulzfeld, Germany) were kept under standard conditions and fed standard chow ad libitum (Glen Forrest, Western Australia; RM1-E, Special Diet Service, UK). The experimental

protocols were approved by the ethics committee of the Sydney Local Health District Animal Welfare Committee (Approval 2017/012A) and National Animal Research Authority at the Norwegian Food Safety Authority (Mattilsynet; Approval IDs: 4001, 8455, and 0817). All experiments were performed in accordance with relevant approved guidelines and regulations, and reported in accordance with ARRIVE guidelines.

Rats (body weight 300–400 g, age 2–3 months, 8 animals in total) were anesthetized with a mixture of 10 mg/kg Xylazine (Bayer Health Care, California, USA) and 100 mg/kg ketamine (Ketalar, Pfizer, New York, USA), and LSEC were isolated and purified as described Smedsrød et al.[46]. Several fractions of cells were frozen and prepared as described previously[47].

Reagents included caffeine (Cat No. C0750; Sigma-Aldrich, Oslo, Norway), theobromine (Cat No. T4500; Sigma-Aldrich, Oslo, Norway), theophylline (Cat No. T1633; Sigma-Aldrich, Oslo, Norway), and paraxanthine (Cat No. P6148; Sigma-Aldrich, Oslo, Norway). Fibronectin was isolated from human plasma using Gelatin-Sepharose 4B (Cat No. 17-0956-01, GE Healthcare, Sydney, Australia) according to the manufacturer's instructions. All reagents were dissolved in serum-free RPMI media (Sigma-Aldrich, Sydney, Australia; Oslo, Norway). All experiments were performed in triplicate, using cells isolated from three different rats. In vitro treatment of LSEC with caffeine was at 8 and 150 µg/mL. Metabolites of caffeine: theobromine (8 and 150 µg/mL), theophylline[40] (20 and 150 µg/mL), paraxanthine (8 and 150 µg/mL) were applied at physiologically relevant and high concentrations in the same manner as for caffeine. For the dose–response study, rat LSEC were treated with caffeine at concentrations: 1, 8, 50, 150, 250 and 500 µg/mL.

Scanning electron microscopy (SEM). For SEM preparation, the thawing and LSEC culturing protocols are described elsewhere[47]. Cells were plated on 0.2 mg/mL fibronectin coated coverslips and cultured (37 °C, 5% CO_2) for 3 h in serum-free RPMI-1640 (with 10,000 U/mL Penicillin, 10 mg/mL Streptomycin, 1:100) (Sigma-Aldrich, Sydney, Australia) at a density of 0.2×10^6 cells/cm^2. The LSEC were treated with various agents for 30 min to determine their effects on fenestrations. The choice of a 30-min treatment duration was based on the reported plasma concentration–time curves where peak concentration of xanthines after digestion of xanthine containing food/beverages are observed at 30–60 min. The shortest but physiologically relevant time was chosen to avoid the effect of primary LSEC morphological changes in vitro. Then the samples were fixed using McDowell's solution (4% formaldehyde and 2.5% glutaraldehyde in PHEM buffer pH 7.2) for 15 min and stored in McDowell's solution until preparation for SEM. After washes with PHEM, the coverslips containing the cells were treated with freshly made 1% tannic acid in 0.15 mol/l PHEM buffer for 1 h, 1% OsO_4 in water for 1 h, dehydrated in ethanol (30%, 60%, 90% for 5 min each, 5 times 100% ethanol for 4 min each), and incubated twice in hexamethyldisilazane for 2 min (Sigma-Aldrich, Oslo, Norway), before coating with 10-nm gold/palladium alloys. Imaging and image analysis was performed blind to the sample ID. Coded specimens were examined using a commercial SEM (Sigma HV0307 or Gemini 300, Zeiss) at 2 kV. Large fields of view (magnification of 1k) containing several/individual cells were randomly acquired to determine cell culture condition and cell size, and high-resolution SEM images of cell at magnification of 15k were selected blindly to assess fenestration size.

Fenestration size, porosity and frequency were assessed in SEM images from each cell culture selected from different areas. Open pores with diameters between 50 and 350 nm were defined as fenestrations and holes larger than 350 nm as gaps. Porosity was defined as the sum area of fenestrations per total area of the cell in the micrographs. Frequency was denoted as the total number of fenestrations per sum area of the cell excluding the sum area of gaps[48].

Structured illumination microscopy (SIM). After fixation, the cells were stained with CellMask Green (1:1000 in phosphate buffered saline (PBS)) for 10 min, washed three times in PBS and then mounted in Vectashield antifade mounting medium (Vectro Laboratories, Burlingame, California) and imaged using a commercial super-resolving SIM (DeltaVision/OMXv4.0 BLAZE, GE Healthcare) with a 60× 1.42 NA oil-immersion objective (Olympus). 3D-SIM image stacks of 1 µm were acquired with a z-distance of 125 nm and with 15 raw images per plane (five phases, three angles). Raw datasets were computationally reconstructed using SoftWoRx software (GE Healthcare). The datasets were further analyzed using the pixel classification workflow in the freely available machine learning image processing software Ilastik[49]. Fenestration detection steps were described in our previous study[50]; notably, the detected objects with diameters below 50 nm and above 300 nm were excluded prior to binning for SIM images.

Endocytosis and degradation assay. For quantitative studies of endocytosis and degradation, fully confluent cultures of rat LSEC (approximately $0.25–0.3 \times 10^6$ cells/cm^2) were established in 48-well culture dishes coated with fibronectin, were pretreated with different agents for 30 min (at 37 °C, 5% CO_2), subsequently incubated in 0.2 mL serum-free RPMI containing 1% human serum albumin and ~ 20,000 cpm ^{125}I-FSA (formaldehyde-treated serum albumin) for 2 h (total incubation time with drugs was 2.5 h). Thereafter, the cell-associated and degraded FSA fractions were analyzed as described previously[51,52]. Briefly, LSEC scavenge ^{125}I-FSA via the endocytic cell surface receptors stabilin-1 and -2, and this is later digested, resulting in the separation of FSA and ^{125}I (free iodine). The degraded fraction was calculated from the measurement of free iodine in the supernatant solution after precipitation of the remaining intact ^{125}I-FSA using 20% trichloroacetic acid. The cell-associated fraction was measured after lysis of the cells with 1% sodium dodecyl sulfate (SDS). The data was analyzed after subtraction of the unspecific binding and free iodine content in the cell free controls. The radioactivity was measured using a Cobra II, Auto-Gamma detector (Packard Instruments, Laborel, Oslo, Norway).

Data analysis and statistics. We selected image analysis methods according to our previous study[48]. Fenestration diameters were measured from SEM images using a threshold-based semi-automated method. This

approach allowed us to greatly improve both the number of analysed fenestrations as well as the precision of measurement. Mean fenestration diameters were calculated from the single fenestration areas obtained from the segmented images (see supplementary information Fig. S1). Fenestration frequency was obtained from the manually counted fenestrations from each cell. This reduced the influence of any imaging artifacts including differences in image quality between the samples. Porosity was calculated as a combination of both fenestration number and size distribution (details can be found in the supplementary information of ref.[48]).

All graphs were prepared using OriginPro software (OriginPro 2021, OriginLab Corp., Northampton, Massachusetts) and image analysis was performed using the free, open-source software Fiji/Image J[53]. Significance was assessed using a two-tailed student T-test for porosity and fenestration frequency parameters. Fenestration diameters and endocytosis experimental data were analyzed with one-way ANOVA performed using the GraphPad Prism 8 (La Jolla, USA, https://www.graphpad.com), and the post hoc tests were used with Dunnett's multiple comparisons test for each treatment with control. The results were considered significant if $p < 0.05$ (*) or described as trends for $p < 0.1$ (#).

Results and discussion

Dose-response of LSEC treated with caffeine. A typical flat, well-spread morphology was observed in all samples, and cell culture purity was assessed based on the presence of the unique morphological feature of LSEC—fenestrations (Fig. 2). SEM data with the analyzed number of cells as well as fenestration diameter, porosity (i.e. percentage of the cell surface covered by fenestrations) and frequency (i.e. the number of fenestrations per cell area) following various treatments are summarized in Table 1. The fenestration diameter after treatment remains within the range of 160 to 180 nm, which is consistent with previously reported data[23,24]. Roughly 20,000–50,000 "holes" were analyzed for each treatment group to calculate fenestration diameters. Fenestration frequency and porosity were measured for ~ 35 cells total from three individual animals.

Changes in fenestration size in combination with differences in fenestration number may also influence the average cell porosity. Fenestration frequency is a parameter describing the number of fenestrations per cell which in combination with fenestration size can be translated into porosity—the percentage of the cell area covered in fenestrations. The diameter of fenestrations is responsible for (size-dependent) selectivity of passive transport between the bloodstream and hepatocytes, while the number of fenestrations per cell/area relates to the rate of liver filtration[54].

To better understand the effect of caffeine, a dose-dependent study was performed using SEM images. A decrease in fenestration diameter was observed for concentrations of 50–250 µg/ml, reaching the minimum at 166 nm at 150 µg/ml (in comparison with 176 nm in the untreated cells) (Table 1, Fig. 3A). For the highest used concentration of 500 µg/ml, a small increase in the diameter was observed. The analysis of the fenestration number showed a dose-dependent increase in the fenestration frequency for caffeine concentrations of 8 µg/ml or above (Fig. 3B). The highest value of 2.9 fenestrations per μm^2 was reached at the caffeine concentrations of 250 µg/ml, which is an over two-fold increase compared with the control. No further increase in fenestration frequency was observed. Similar trends were observed for the porosity parameter calculated from the

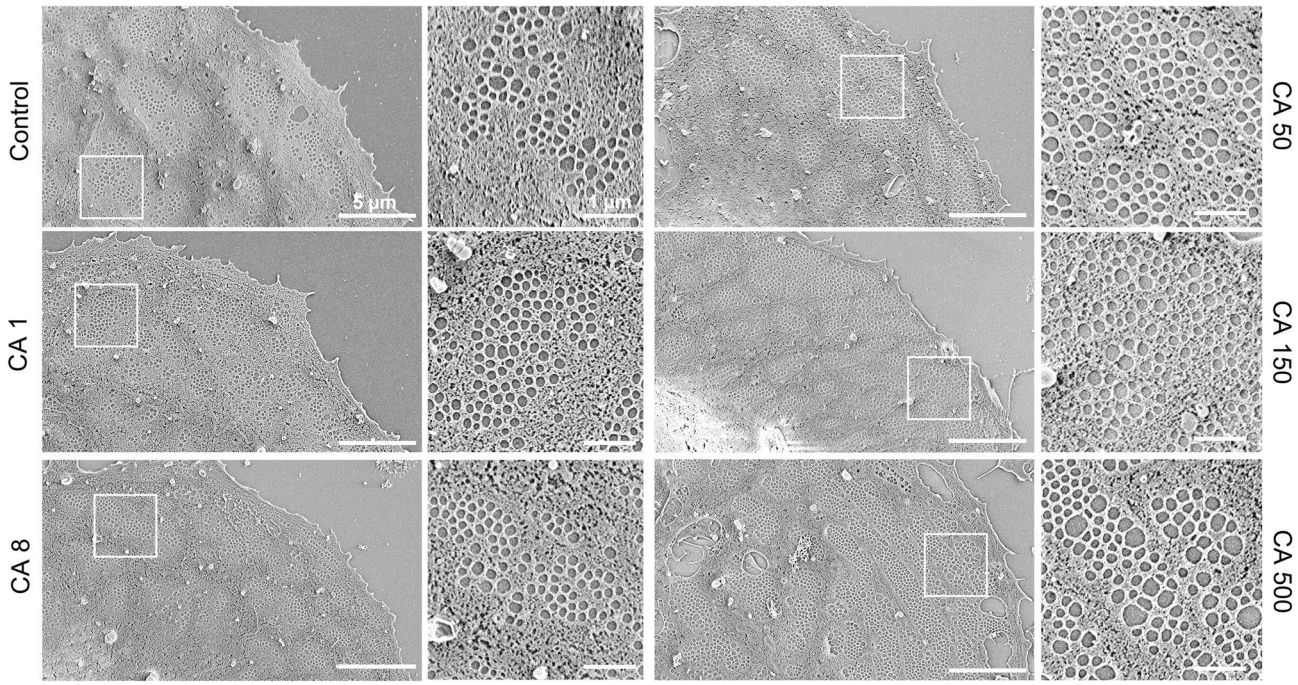

Figure 2. Representative scanning electron microscopy (SEM) images following 30 min of caffeine treatment of rat liver sinusoidal endothelial cell (LSEC) fenestrations. Scale bar size: overview images 5 µm, inset 1 µm. *CA* caffeine, indicated concentrations are µg/mL.

Concentration (µg/mL)	No. fenestrations measured	Diameter (nm) ± HWHM	Frequency (no./µm²) ± SD	Porosity (%) ± SD	No. cells measured
Control	19,811	176 ± 33	1,25 ± 0.49	3.13 ± 1.23	35
1	35,999	178 ± 35	1,62 ± 0.99	3.74 ± 2.28	35
8	51,571	177 ± 36	1,97 ± 0.80**	5.03 ± 2.04**	33
50	46,041	170 ± 36*	2,09 ± 1.16**	4.84 ± 2.68**	34
150	52,370	166 ± 33*	2,42 ± 0.81**	5.57 ± 1.87**	32
250	41,741	170 ± 34*	2,85 ± 0.81**	6.77 ± 1.93**	34
500	23,998	179 ± 36	2,54 ± 0.83**	6.39 ± 2.10**	34

Table 1. Changes in the parameters describing fenestrated morphology of freshly isolated LSEC after treatment with caffeine. Measurements were extracted from SEM images using semi-automatic (diameter) and manual methods (frequency). *HWHM* half-width at half maximum, *SD* standard deviation. *p < 0.05, **p < 0.01.

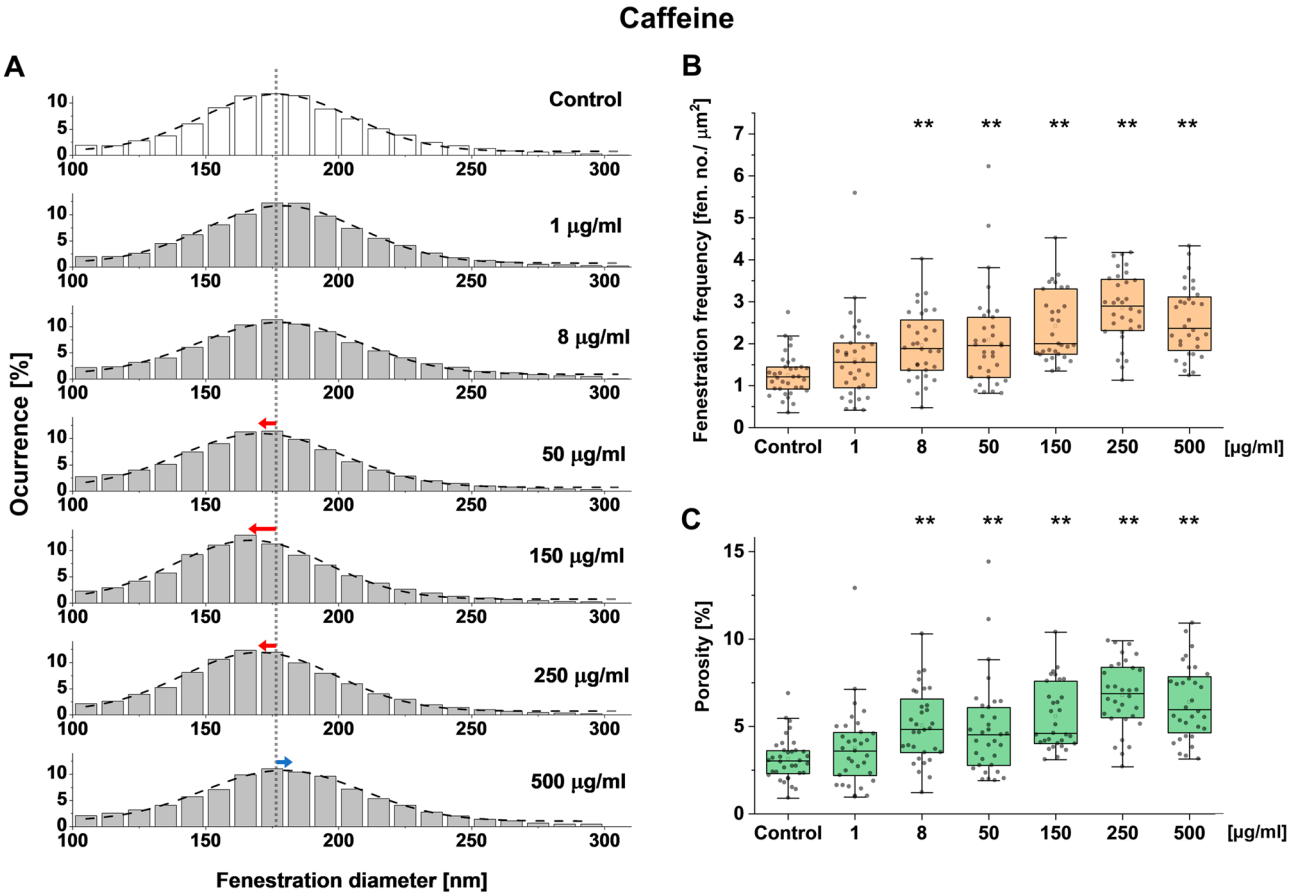

Figure 3. Dose response of LSEC treated with caffeine and changes in fenestration diameter distribution (**A**), fenestration frequency (**B**) and porosity (**C**). (**A**) Dotted line indicates the mean fenestration diameter of the untreated group and arrows show the trends of changes in diameter in the treatment groups. ** p<0.01

combination of fenestration frequency and diameter data (Fig. 3C). Interestingly, the comparison of porosity data for different treatments shows a connection between fenestration size and number. For example, no change in fenestration frequency was observed between the caffeine concentrations of 8 and 50 µg/ml, while a 7 nm decrease in the mean fenestration diameter led to a reduction in porosity from 5.0 to 4.8%. Similarly, a 13 nm increase in the mean fenestration diameter between the treatments of 150 and 500 µg/ml resulted in an increase in porosity from 5.6 to 6.4%.

The effects of other xanthines on LSEC morphology. Caffeine is metabolized in the liver into three main metabolites: theobromine, theophylline and paraxanthine (Fig. 1)[11,12]. Here we study and compare the effects of those xanthines on LSEC. Similarly to the caffeine dose response experiment, we observed typical flat, well-spread morphology in all samples (Fig. 4). SEM data with the analyzed number of cells as well as

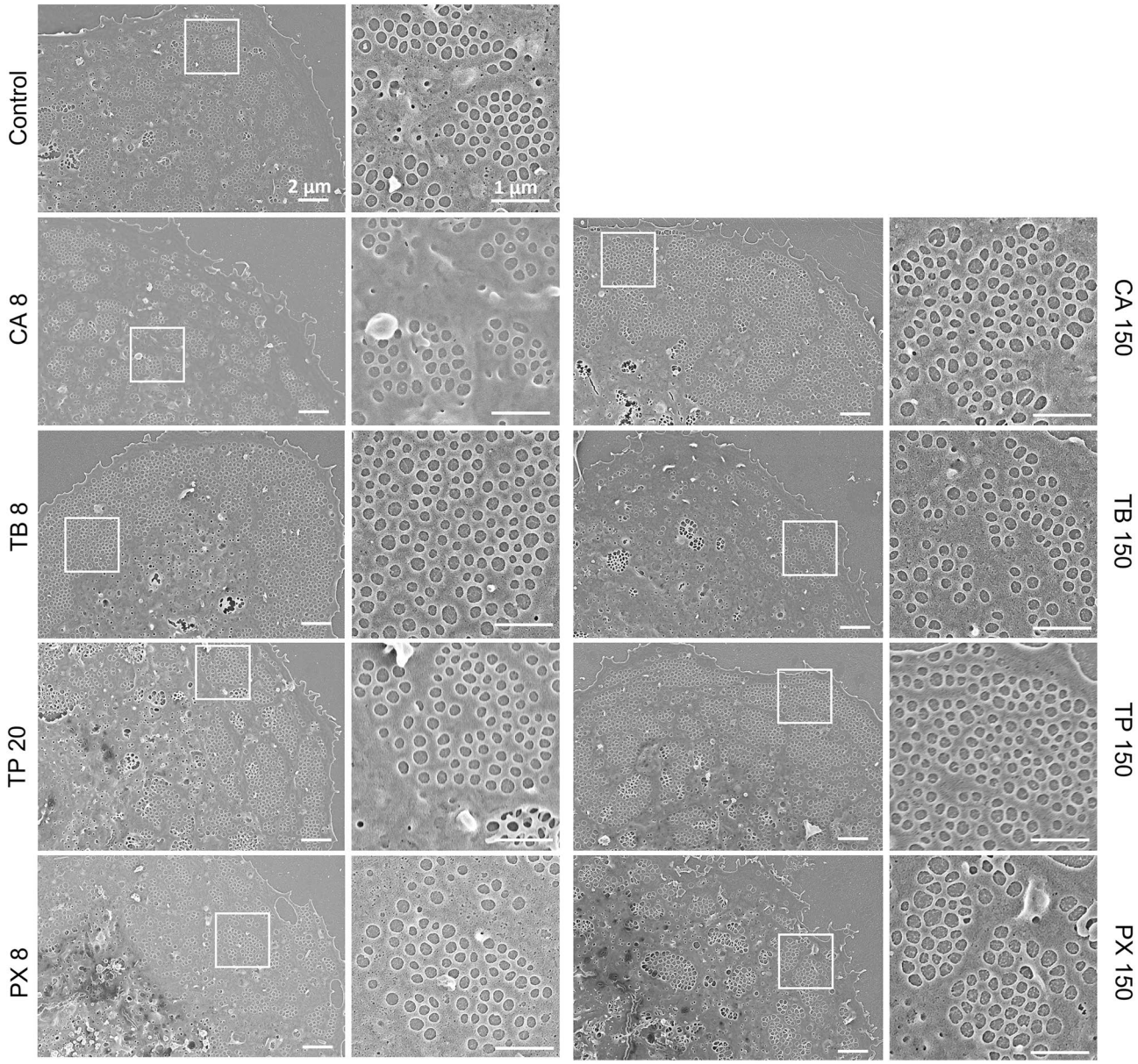

Figure 4. Representative scanning electron microscopy (SEM) images following xanthines treatment of rat liver sinusoidal endothelial cell (LSEC) fenestration. Scale bar size: overview images 2 µm, inset 1 µm. *CA* caffeine, *TB* theobromine, *TP* theophylline, *PX* paraxanthine. Indicated concentrations are µg/mL.

fenestration diameter, porosity and frequency following xanthine treatments are summarized in Table 2. Roughly 7200–69,000 fenestrations were analyzed for each treatment group to calculate fenestration diameters. Fenestration frequency and porosity were measured for around 60 cells total from 3 individual animals.

The cell morphology from different treatment groups was observed after 30 min incubation. No drastic changes and signs of toxicity were noticed. Only the high dose (150 µg/mL) of theobromine showed possible early signs of toxicity in some cells—namely irregular cell edges and shrinking.

Quantitative effects on fenestrations. Some of the xanthines elicited changes in the fenestration frequency (Fig. 5, Table 2): a significant increase was observed for the high doses (150 µg/mL) of caffeine, theophylline and lower dose (8 µg/mL) of theobromine, (increase in number by 0.55, 0.71 and 0.80 fenestrations per μm^2, respectively). Also, high doses of theobromine and paraxanthine show increasing trends in fenestration number. The less prominent effect of high versus low dose of theobromine may be a result of early toxic effects suggested by the visual examination of the cell images—some cells treated with the high dose showed signs of irregular cell edges or reduced cell area. The trend after paraxanthine treatment may suggest that exposure to the drug longer than the incubation time used here (30 min) may further increase LSEC porosity. In humans, paraxanthine is the main metabolite of caffeine and its concentration in the plasma can reach higher values than caffeine itself and remain at this high level for prolonged periods, up to a few hours[17].

Treatment		No. fenestrations measured	No. cells (for diameter)	Diameter (nm) ± HWHM	Frequency (no./μm²) ± SD	Porosity (%) ± SD	No. cells measured (for frequency)
Drug	Concentration (μg/mL)						
Control	–	68,829	157	197 ± 48	2.52 ± 1.33	7.50 ± 4.24	51
Caffeine	8	7235	33	179 ± 45*	2.72 ± 1.27	7.04 ± 3.27	49
	150	18,844	34	187 ± 49*	3.07 ± 1.38*	9.13 ± 3.91*	60
Theobromine	8	12,771	20	192 ± 40*	3.32 ± 1.42*	7.50 ± 3.29	55
	150	7029	17	188 ± 61*	3.15 ± 1.43#	7.65 ± 3.48	49
Theophylline	20	13,496	27	195 ± 42	2.61 ± 1.14	8.15 ± 3.36	54
	150	20,311	33	180 ± 43*	3.23 ± 1.39*	8.97 ± 3.45#	60
Paraxanthine	8	15,210	21	182 ± 42*	2.80 ± 1.28	8.61 ± 3.71#	60
	150	16,766	36	198 ± 49	2.88 ± 1.40#	8.79 ± 4.27#	56

Table 2. Changes in the parameters describing LSEC fenestrated morphology. Measurements were extracted from SEM images using semi-automatic (diameter) and manual methods (frequency). *HWHM* half-width at half maximum, *SD* standard deviation. *$p < 0.05$, #$p < 0.1$.

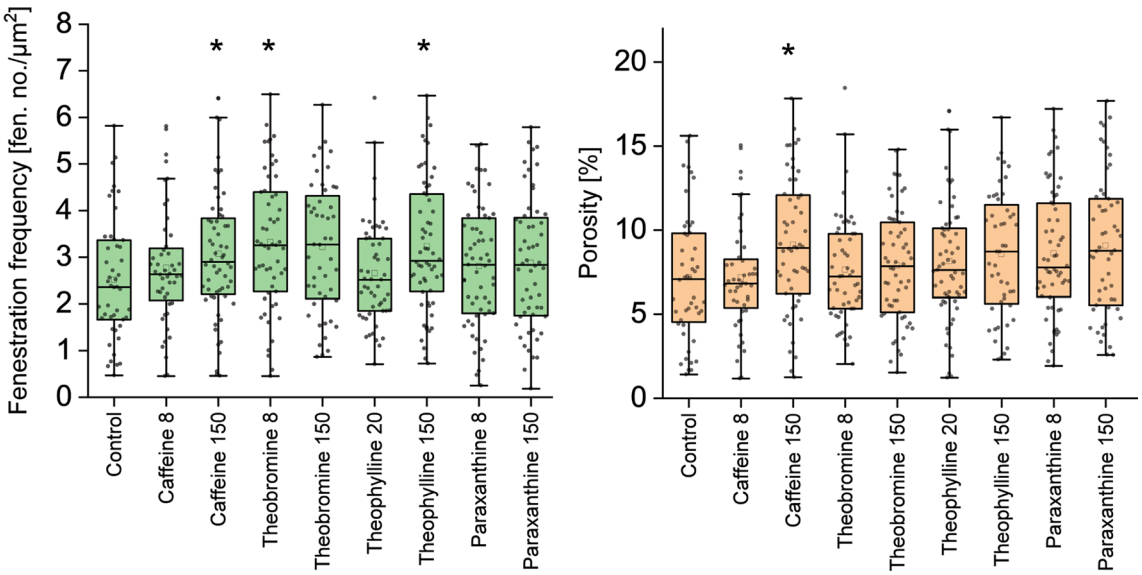

Figure 5. Fenestration frequency and porosity of LSEC treated with xanthines. The graphs present combined data from 3 studied animals. Treatment concentrations are indicated in μg/ml. Each dot represents analyzed SEM image of a single cell. *$p < 0.05$.

Even though we did not observe large changes in the mean fenestration diameters, the porosity parameter shows the influence of the diameter distribution (Table 2). A significant increase (22%) in porosity was observed only in the high dose of caffeine. The high dose of caffeine did not affect the mean fenestration diameter, so the effect is visible in both parameters. On the other hand, high doses of both theobromine and theophylline caused a decrease in fenestration size which counteracted the influence of increased fenestration number. In vivo, such an occurrence would suggest more rapid filtration of the smaller molecules in the liver. Paraxanthine for both concentrations and high dose theophylline treatments also showed an increasing trend in porosity.

To further understand the changes in fenestration diameter after the various treatments, we studied the whole distribution of fenestration size, instead of just average values. We observed shifts in the diameter histograms, and to better visualize that data we separated fenestrations into three size groups: small (S)— < 100 nm, medium (M)—100–200 nm, large (L)— > 200 nm. These groups can be related to the filtration of different molecules that are metabolized by hepatocytes—HDL and LDL have a diameter below 100 nm, while chylomicron remnants are usually above 100 nm in diameter[55]. Already in 1970, Wisse pointed out that fenestration size may play a role in liver filtration[20] and later in 1995, Fraser et al.[56] proposed the barrier function of LSEC that is chylomicron remnant clearance, namely that LSEC fenestration diameter dictates which chylomicron remnants can be removed from the circulation. Although the filtration function of LSEC is a combination of both passive filtration and active receptor-mediated trans- and/or endocytosis, the previous studies suggest that transportation of lipoprotein fractions through the endothelial barrier is mostly influenced by the passive flow through the fenestrations[57,58]. Changes in the distribution of fenestrations between those groups relative to control can be found in Fig. 6.

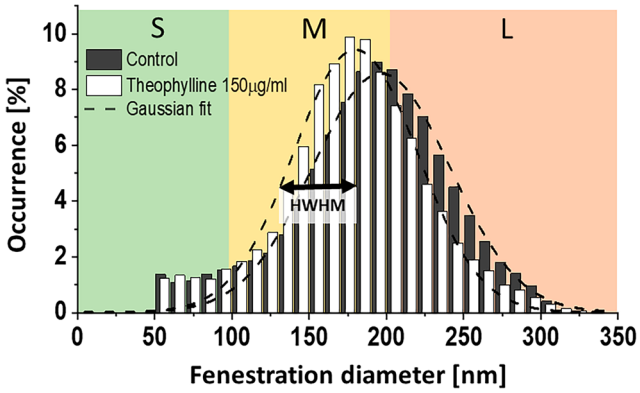

Changes in the distributions of fenestration diameter

Treatment	Dose [µg/ml]	Fenestration diameter			
		S (<100 nm)	M (100-200nm)	L (>200nm)	Gaussian mean ± HWHM
Caffeine	8	2.9% ↑	28.6% ↑	37.8 ↓	179 ± 45*
	150	48.3% ↑	9.4% ↑	21.9% ↓	187 ± 49*
Theobromine	8	1.5% ↑	11.6% ↑	15.5% ↓	192 ± 40*
	150	94.5% ↑	2.4% ↓	14.8% ↓	188 ± 61*
Theophylline	20	6.6% ↑	3.7% ↑	6.7% ↓	195 ± 42
	150	1.3% ↑	25.0% ↑	33.5% ↓	180 ± 43*
Paraxanthine	8	4.2% ↓	26.3% ↑	33.7% ↓	182 ± 42*
	150	22.6% ↑	5.3% ↓	1.9% ↑	198 ± 49
Control	-	-	-	-	197 ± 48

HWHM – half width at half maximum

Figure 6. Fenestration distribution in LSEC treated with xanthines. The graph presents the control group and theobromine (high concentration) treatment as an example (all histograms can be found in supplementary materials (Fig. S2). S (small)/M (medium)/L (large) represent the fractions of fenestrations according to their size. Changes in the fenestration distribution are presented in the table as relative to the control/untreated samples. Gaussian mean is calculated as a center of Gaussian fit. The data was obtained from SEM images using semi-automated method.

We observed a decrease in the large fenestrations after treatment with all xanthines with the exception of the high paraxanthine dose. The high dose of theophylline and lower dose of paraxanthine showed a 33% decrease in the number of large fenestrations. The high dose of caffeine also was responsible for an almost 22% reduction in the large fenestration number. The medium size fenestration fraction was increased by low doses of caffeine and paraxanthine and a high dose of theophylline by 29%, 26% and 25%, respectively. The remaining treatments show little to no effect in this size range. Interestingly, high doses of caffeine and theobromine cause a large increase in the detectable number of small fenestrations, of 48% and 95%, respectively. The high dose of paraxanthine also resulted in a 23% increase in small fenestrations, but unlike caffeine or theobromine it had very little impact on either medium or large pores.

The detailed analysis of the fenestration size distribution reveals some additional information about the changes in the liver sieve (all histograms can be found in supplementary materials (Fig. S2)). To date, most studies reported changes in fenestration size as just a difference in the mean value but a Gaussian-like distribution of fenestration was confirmed in multiple studies[26,48,59]. Here, we show that the fenestration distribution shape can remain as a Gaussian distribution with little to no changes to the mean value while changes in specific fractions, reflected in the distribution width, can be significant and have biological implications. For example, low dose paraxanthine results in over 20% increase in < 100 nm fenestrations with only 5% increase in medium-size holes without a change in the mean fenestration value—197 nm and 198 nm in control and after treatment. Meanwhile, such a change in vivo can lead to increased availability of VLDL, HDL and other small molecules to hepatocytes, therefore increasing filtration from the bloodstream. On the other hand, a decrease in the large fenestration fraction (such as after low doses of caffeine and paraxanthine or high dose of theophylline) can lead to reduced filtration of some fractions of larger chylomicron remnants. Changes in transportation between plasma and hepatocytes can therefore have both positive and negative effects. Lower filtration can have a protective role against reducing the exposure of some agents to hepatocytes, but it also can increase lipoprotein fractions in the blood which may contribute to cardiovascular diseases. Wright et al.[60] showed that smaller liver fenestrations observed in rabbits can be a cause of their susceptibility to arteriosclerosis. This theory is supported by the increase of fenestration size in rabbits reported after pantethine treatment, which reduced their sensitivity to dietary cholesterol[61]. The chylomicron remnant size varies from 100 to even 1000 nm, so the reduction in large or medium fenestrations could correspondingly affect/lower the filtration of certain fractions of chylomicrons containing different amounts of triglycerides and cholesterols.

To validate our findings, we also assessed the fenestrations with some treatments on SIM (Fig. 7, caffeine 150 µg/mL and theophylline 30 µg/mL are shown for comparison). Similar to the SEM observations, LSECs featured numerous fenestrations which were clustered as sieve plates. Further assessment of the diameter of fenestrations was conducted in a machine learning assisted workflow, as was used in a previous study[50]. By comparing the mean fenestration diameter in our dehydrated SEM result with wet-fixed SIM data, the latter resulted in a 15% smaller size for the control groups[62]. The SIM data confirmed the increase in fenestration frequency and changes in diameter distribution induced by the high dose of caffeine and theophylline (Fig. 7).

Though not having as high resolution as SEM, the SIM technique gives a resolution double that obtained via conventional light microscopy. The average diameter of fenestrations is well discerned within the regular observed size range. For SIM, the samples can be studied while wet, thus avoiding the artifacts from dehydration required for SEM. 3D-SIM was used in our study to image fenestrations in fixed rat LSECs in Vectashield mounted samples. Importantly, a limitation of the linear SIM is that only fenestrations with a diameter around 100 nm or more are resolved. As mentioned above, by comparing the results of the control group from both methods, the mean fenestration diameter was larger in SEM processed samples, which might be due to the dehydration step during

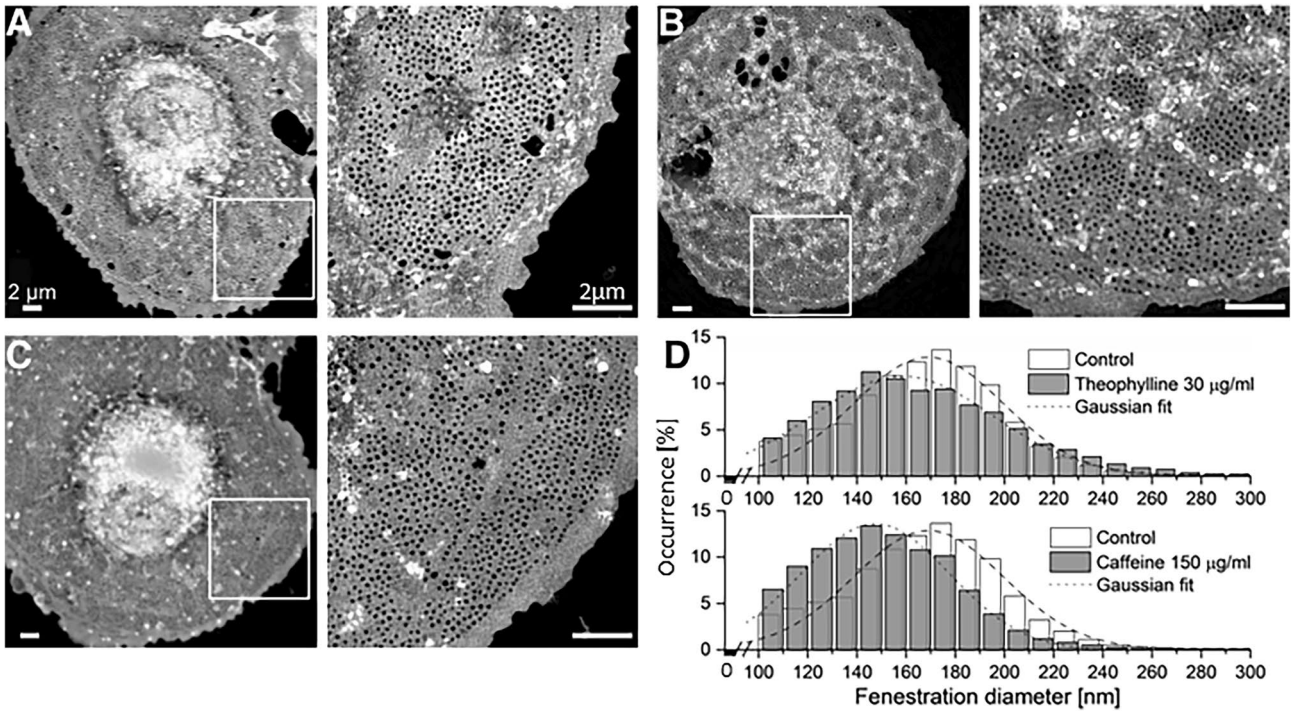

Figure 7. Maximum intensity z-projections of 3D-SIM images show fenestrations grouped in sieve plates (inset) following treatments. (**A**) Control; (**B**) theophylline (30 µg/mL); (**C**) caffeine (150 µg/mL); (**D**) fenestration size distribution after treatments. Mean diameter calculated from Gaussian fits ± HWHM (half-width at half maximum): control 169 ± 35 nm, theophylline 159 ± 43 nm, caffeine 148 ± 35 nm. All scale bars (including insets): 2 µm.

SEM preparation. Notably, due to the resolution limit of SIM being around 100 nm, the diameter analyzed from SIM images was of the same magnitude (Fig. 7D).

Xanthines effect on LSEC viability. LSEC are the main scavenger cells in the body, clearing various compounds from the blood[18]. A well-established method for validation of LSEC functional viability is a measurement of their endocytic capacity of denatured or modified proteins such as formaldehyde-treated serum albumin (FSA)[63]. To assess the possible toxic effects of xanthines, we measured the uptake and degradation of radiolabeled FSA in LSEC (Fig. 8). The data show no effects on endocytosis after caffeine treatment (up to 1500 µg/ml). Theobromine showed an 8% decrease in total endocytosis at 250 µg/ml, while theophylline and paraxanthine showed 10% and 8% reduction, respectively, at 1500 µg/ml. Evaluation of cell morphology on SEM images did not reveal any apparent morphological disruptions characteristic for LSEC (Fig. 4) (indicated by e.g., large gaps > 400 nm, cell shrinkage or disrupted cell edges). The additional morphological assessment was performed using SIM (Fig. 7). Nevertheless, this small decrease of degradation of FSA could be related to the toxic effects of the compounds. We did not reach in vitro toxic concentration of caffeine and the negative effects of other xanthines were observed only at very high concentrations of 250/1500 µg/mL which are above the reported in vivo toxic doses[36].

Possible mechanisms of action. Caffeine is metabolized in hepatocytes mainly by the CYP1A2 enzyme and the exons for this enzyme vary between humans[64]. These differences cause variations in caffeine metabolism which affects clearance time and therefore results in the different total stimulating effects of caffeine. LSEC do not express CYP1A2[65] nor metabolize caffeine per se, however, here we show that xanthines can affect their morphology. The exact mechanism is not known but there are several receptors and pathways present in LSEC that can be affected. Based on our extensive review of mechanisms behind the structure and functioning of LSEC fenestration, some possible mechanisms of action can be proposed[24].

For example, changes in intracellular cGMP can be associated with fenestration regulation. Hunt et al.[27] showed that drugs promoting cGMP and PKG, such as sildenafil, have positive effects on porosity and fenestration frequency. cGMP levels are mainly controlled by the regulation of its degradation by various phosphodiesterases (PDE) as well as by extracellular efflux by ABC transporters[66]. Both caffeine and theophylline were reported to act as non-specific PDE inhibitors[66,67]. This data suggest the possible mechanism of action via the cGMP-PKG pathway, however further studies are necessary to confirm this.

Caffeine and paraxanthine can also act through nonselective antagonizing of adenosine receptors[68], which could influence fenestrations via reduction of cAMP. A decrease of cAMP resulting from serotonin challenge showed a decrease in the fenestration size[30], similar to the observed here after treatment with a high concentration

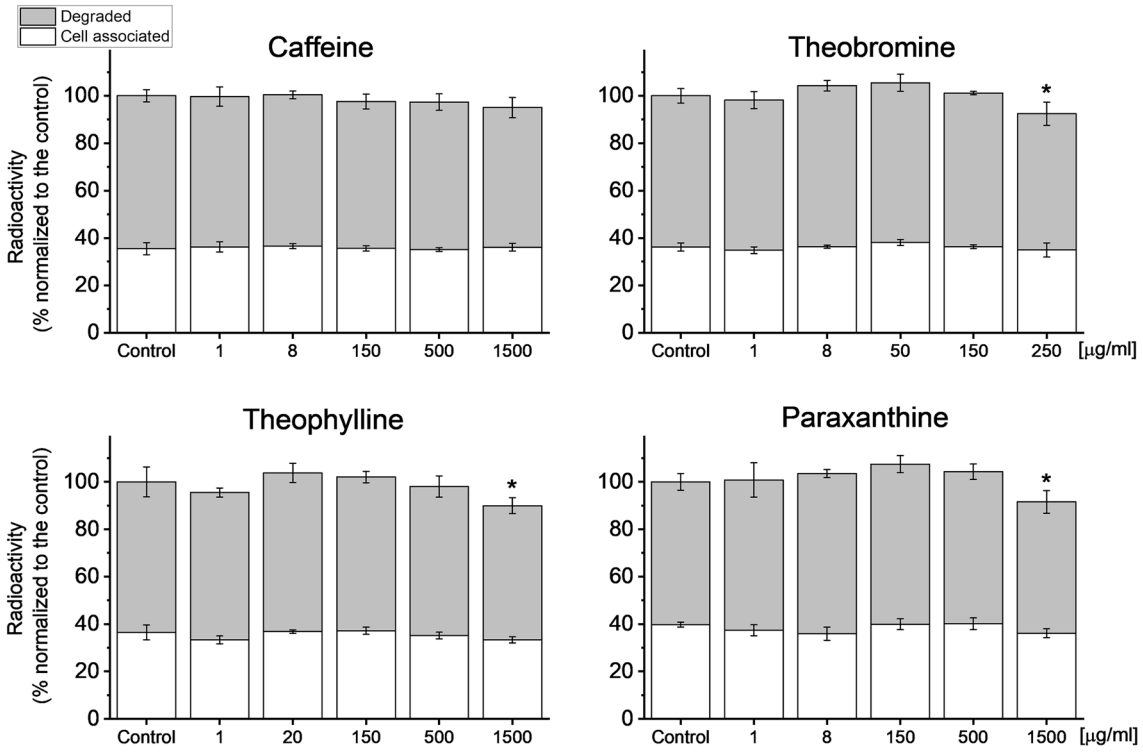

Figure 8. ^{125}I-FSA uptake in isolated LSEC after treatments with xanthines. Incubation time with ^{125}I-FSA—2 h. Bars indicate mean ± SD, n = 3, *p < 0.05.

of xanthines. This mechanism has not been confirmed in LSEC yet, however, the effects of adenosine receptors in the liver are currently under investigation[69].

Translational relevance. The physiologically achievable non-toxic plasma concentrations of xanthines in humans are up to about 1–8 µg/mL. The endocytosis data show that xanthines have no negative effects in this concentration range. The decrease in the LSEC endocytic activity was observed only with very high concentrations of theobromine, theophylline and paraxanthine which are not physiologically relevant. The decrease in FSA endocytosis is due to reduced degradation, not uptake, which suggests a possible influence of high concentrations of xanthines on the lysosomal degradation or intercellular transportation, rather than an influence on the scavenging receptors. Together with the LSEC morphology results, it suggests that there is no correlation between the cell porosity and endocytic activity, which agrees with the report of Simon-Santamaria et al.[63].

Daily consumption of 40–80 g of dark chocolate or 110 g of regular milk chocolate yields a plasma theobromine concentration of 4–8 µg/mL in humans, which is within the region that elicits increased porosity in rat LSEC in vitro. Our study demonstrated theobromine, at physiologically relevant concentrations, may increase the fenestration frequency in LSEC, which may further affect hepatocyte metabolism and xenobiotic detoxification. If the results in this study translate to the in vivo context, the theobromine induced increase in fenestration number could improve liver function by enhancing the bi-directional exchange of substrates between the plasma and the hepatocytes, for example in the elderly who have reduced LSEC porosity. On the other hand, due to fenestration loss associated with ageing, some hepatocyte-targeting drug dosages should be adjusted for elderly people[70]. The otherwise positive effect or re-fenestration (induced reappearance of fenestrations) after xanthine treatment could lead to toxic effects due to the sudden increase of drug levels to which hepatocytes are exposed. This effect may be even more relevant for the people taking multiple drugs at the time as polypharmacy (daily intake of 5 or more drugs) is steadily increasing in recent years[71].

The positive effects of high doses of caffeine and theophylline are however harder to translate into useful intervention for the benefit of liver health as this concentration (150 µg/mL) is within the toxic range for those compounds. Recent studies have suggested the high plasma concentration needed for effect can be avoided if therapies are directly delivered to LSECs via nanoparticles and may result in similar in vivo effects as observed in vitro[72,73]. Further studies are clearly required to determine if xanthines affect fenestrations in vivo. Previous studies investigated the possibility of using rates of caffeine clearance as a guide to deteriorating liver function in cirrhosis. The results could be explained by the effect on LSEC fenestrations as the caffeine clearance did not correlate with conventional liver function tests[37]. These findings suggest that the development of the new tests of hepatic function should take into consideration also possible effects of the agents on the LSEC barrier, and not only hepatocyte metabolism.

Conclusions

In conclusion, we have shown in vitro xanthine treatments with caffeine, theobromine, theophylline and paraxanthine elicit changes in fenestration size, porosity and frequency in rat LSEC. It is only at very high concentrations, that xanthines have an inhibitory impact on the uptake of soluble macromolecules. Caffeine and theophylline in high doses increase fenestration frequency and the number of smaller-sized fenestrations in LSEC. Theobromine at a physiologically relevant dose (achievable e.g., after consumption of food with high cocoa content) also increases fenestration frequency in rat LSEC. Although similar findings remain to be confirmed in vivo, if theobromine elicits these effects in animal studies, it might prove to be a useful intervention to improve LSEC porosity in elderly people. Concomitant to this, caffeine and theophylline could be used for the improvement of LSEC fenestration number; however, a drug delivery system targeting LSEC would be required to avoid unwanted systemic side effects.

Data availability

The datasets generated and analysed during the current study are not publicly available due to their large file size but are available from the corresponding author on reasonable request.

Received: 24 March 2023; Accepted: 7 August 2023
Published online: 17 August 2023

References

1. Heckman, M. A., Weil, J. & de Mejia, E. G. Caffeine (1, 3, 7-trimethylxanthine) in foods: A comprehensive review on consumption, functionality, safety, and regulatory matters. *J. Food Sci.* **75**, 77–87. https://doi.org/10.1111/j.1750-3841.2010.01561.x (2010).
2. Pini, L. A. *et al.* Tolerability and efficacy of a combination of paracetamol and caffeine in the treatment of tension-type headache: A randomised, double-blind, double-dummy, cross-over study versus placebo and naproxen sodium. *J. Headache Pain* **9**, 367–373. https://doi.org/10.1007/s10194-008-0071-5 (2008).
3. Schachtel, B., Fillingim, J. M., Lane, A. C., Thoden, W. R. & Baybutt, R. I. Caffeine as an analgesic adjuvant a double blind study comparing aspirin with caffeine to aspirin and placebo in patients with sore throat. *Arch. Intern. Med.* https://doi.org/10.1001/archinte.151.4.733 (1991).
4. Ward, N., Whitney, C., Avery, D. & Dunner, D. The analgesic effects of caffeine in headache. *Pain* **44**, 151–155. https://doi.org/10.1016/0304-3959(91)90129-L (1991).
5. Antwerpes, S. *et al.* Coffee intake and neurocognitive performance in HIV/HCV coinfected patients (ANRS CO13 HEPAVIH). *Nutrients* https://doi.org/10.3390/nu12092532 (2020).
6. Herden, L. & Weissert, R. The effect of coffee and caffeine consumption on patients with multiple sclerosis-related fatigue. *Nutrients* https://doi.org/10.3390/nu12082262 (2020).
7. Hong, C. T., Chan, L. & Bai, C. The effect of caffeine on the risk and progression of Parkinson's disease: A meta-analysis. *Nutrients* https://doi.org/10.3390/nu12061860 (2020).
8. Nowaczewska, M., Wicinski, M. & Kazmierczak, W. The ambiguous role of caffeine in migraine headache: From trigger to treatment. *Nutrients* https://doi.org/10.3390/nu12082259 (2020).
9. Jee, H. J., Lee, S. G., Bormate, K. J. & Jung, Y. S. Effect of caffeine consumption on the risk for neurological and psychiatric disorders: Sex differences in human. *Nutrients* https://doi.org/10.3390/nu12103080 (2020).
10. Arnaud, M. J. Metabolism of caffeine and other components of coffee. *Caffeine Coffee Health* **1993**, 43–95 (1993).
11. Somani, S. & Gupta, P. Caffeine: A new look at an age-old drug. *Int. J. Clin. Pharmacol. Ther. Toxicol.* **26**, 521–533 (1988).
12. Carrillo, J. A. & Benitez, J. Clinically significant pharmacokinetic interactions between dietary caffeine and medications. *Clin. Pharmacokinet.* **39**, 127–153. https://doi.org/10.2165/00003088-200039020-00004 (2000).
13. Sawynok, J. & Yaksh, T. Caffeine as an analgesic adjuvant: A review of pharmacology and mechanisms of action. *Pharmacol. Rev.* **45**, 43 (1993).
14. Arnaud, M.J. Pharmacokinetics and metabolism of natural methylxanthines in animal and man. In *Handbook of Experimental Pharmacology.* Vol. 200. 471–478. ISBN 9783642134425 (2011).
15. Arnaud, M. Comparative metabolic disposition of [1-Me14C] caffeine in rats, mice, and Chinese hamsters. *Drug Metab. Dispos.* **13**, 471–478 (1985).
16. Orrú, M. *et al.* Psychostimulant pharmacological profile of paraxanthine, the main metabolite of caffeine in humans. *Neuropharmacology* **67**, 476–484. https://doi.org/10.1016/j.neuropharm.2012.11.029 (2013).
17. Committee on Military Nutrition Research. *Caffeine for the Sustainment of Mental Task Performance: Formulations for Military Operations*. ISBN 978-0-309-08258-7 (National Academy Press, 2001).
18. Sørensen, K. K. *et al.* The scavenger endothelial cell: A new player in homeostasis and immunity. *Am. J. Physiol.-Regul. Integr. Comp. Physiol.* **303**, 1217–1230. https://doi.org/10.1152/ajpregu.00686.2011 (2012).
19. Bhandari, S., Larsen, A. K., McCourt, P., Smedsrød, B. & Sørensen, K. K. The scavenger function of liver sinusoidal endothelial cells in health and disease. *Front. Physiol.* **12**, 1–23. https://doi.org/10.3389/fphys.2021.757469 (2021).
20. McCuskey, R. S. Morphological mechanisms for regulating blood flow through hepatic sinusoids. *Liver* **20**, 3–7. https://doi.org/10.1034/j.1600-0676.2000.020001003.x (2000).
21. Deleve, L. D. Liver sinusoidal endothelial cells in hepatic fibrosis. *Hepatology* **61**, 1740–1746. https://doi.org/10.1002/hep.27376 (2015).
22. Poisson, J. *et al.* Liver sinusoidal endothelial cells: Physiology and role in liver diseases. *J. Hepatol.* **66**, 212–227. https://doi.org/10.1016/j.jhep.2016.07.009 (2017).
23. Braet, F. & Wisse, E. Structural and functional aspects of liver sinusoidal endothelial cell fenestrae: A review. *Comp. Hepatol.* **1**, 1. https://doi.org/10.1186/1476-5926-1-1 (2002).
24. Szafranska, K., Holte, C. F., Kruse, L. D., McCourt, P. & Zapotoczny, B. The whole story about fenestrations in liver sinusoidal endothelial cells. *Front. Physiol.* https://doi.org/10.3389/fphys.2021.735573 (2021).
25. Wisse, E. An electron microscopic study of the fenestrated endothelial lining of rat liver sinusoids. *J. Ultrastruct. Res.* **31**, 125–150. https://doi.org/10.1016/S0022-5320(70)90150-4 (1970).
26. Wisse, E., de Zanger, R. B., Charels, K., Van Der Smissen, P. & McCuskey, R. S. The Liver sieve: Considerations concerning the structure and function of endothelial fenestrae, the sinusoidal wall and the space of Disse. *Hepatology* **5**, 683–692. https://doi.org/10.1002/hep.1840050427 (1985).
27. Hunt, N. J. *et al.* Manipulating fenestrations in young and old liver sinusoidal endothelial cells. *Am. J. Physiol.-Gastrointest. Liver Physiol.* **316**, G144–G154. https://doi.org/10.1152/ajpgi.00179.2018 (2019).
28. Svistounov, D. *et al.* The relationship between fenestrations, sieve plates and rafts in liver sinusoidal endothelial cells. *PLoS ONE* **7**, 1–9. https://doi.org/10.1371/journal.pone.0046134 (2012).

29. Xie, G. *et al.* Role of differentiation of liver sinusoidal endothelial cells in progression and regression of hepatic fibrosis in rats. *Gastroenterology* **142**, 918-927.e6. https://doi.org/10.1053/j.gastro.2011.12.017 (2012).
30. Gatmaitan, Z. *et al.* Studies on fenestral contraction in rat liver endothelial cells in culture. *Am. J. Pathol.* **148**, 2027–2041 (1996).
31. Zapotoczny, B. *et al.* Tracking fenestrae dynamics in live murine liver sinusoidal endothelial cells. *Hepatology* **69**, 876–888. https://doi.org/10.1002/hep.30232 (2019).
32. Curatolo, P. & Robertson, D. The health consequences of caffeine. *Ann. Intern. Med.* **98**, 641–653. https://doi.org/10.7326/0003-4819-98-5-641 (1983).
33. Nawrot, P. *et al.* Effects of caffeine on human health. *Food Addit. Contam.* **20**, 1–30. https://doi.org/10.1080/0265203021000007840 (2003).
34. Fredholm, B. B., Bättig, K., Holmén, J., Nehlig, A. & Zvartau, E. E. Actions of caffeine in the brain with special reference to factors that contribute to its widespread use. *Pharmacol. Rev.* **51**, 83 (1999).
35. Kulkarni, P. & Dorand, R. Caffeine toxicity in a neonate. *Pediatrics* https://doi.org/10.1542/peds.64.2.254 (1979).
36. Sepkowitz, K. A. Energy drinks and caffeine-related adverse effects. *JAMA-J. Am. Med. Assoc.* **309**, 243–244. https://doi.org/10.1001/jama.2012.173526 (2013).
37. Cheng, W. S. C. *et al.* Dose-dependent pharmacokinetics of caffeine in humans: Relevance as a test of quantitative liver function. *Clin. Pharmacol. Ther.* **47**, 516–524. https://doi.org/10.1038/clpt.1990.66 (1990).
38. Bonati, M. *et al.* Caffeine disposition after oral doses. *Clin. Pharmucol. Ther.* **32**, 98–106 (1982).
39. Blanchard, J., Harvey, S. & Morgan, W. Variability of the serum protein binding of theophylline in patients with asthma and cystic fibrosis. *Br. J. Clin. Pharmacol.* **33**, 653–656. https://doi.org/10.1111/j.1365-2125.1992.tb04096.x (1992).
40. Rowe, D. J. F., Watson, I. D., Williams, J. & Berry, D. J. The clinical use and measurement of theophylline. *Ann. Clin. Biochem.* **25**, 4–26. https://doi.org/10.1177/000456328802500102 (1988).
41. Geib, A.-J. Theophylline and other methylxanthines. In *Critical Care Toxicology: Diagnosis and Management of the Critically Poisoned Patient*. 1–3058. ISBN 9783319179001 (2017).
42. Baggott, M. J. *et al.* Psychopharmacology of theobromine in healthy volunteers. *Psychopharmacology* **228**, 109–118. https://doi.org/10.1007/s00213-013-3021-0 (2013).
43. Mayorga-Gross, A. L. & Esquivel, P. Impact of cocoa products intake on plasma and urine metabolites: A review of targeted and non-targeted studies in humans. *Nutrients* https://doi.org/10.3390/nu11051163 (2019).
44. Mumford, G. K. *et al.* Absorption rate of methylxanthines following capsules, cola and chocolate. *Eur. J. Clin. Pharmacol.* **51**, 319–325. https://doi.org/10.1007/s002280050205 (1996).
45. Resman, B. H., Blumenthal, H. P. & Jusko, W. J. Breast milk distribution of theobromine from chocolate. *Pediatr. Pharmacol. Ther.* **97**, 477–480. https://doi.org/10.1016/S0022-3476(77)81329-2 (1977).
46. Smedsrød, B. & Pertoft, H. Preparation of pure hepatocytes and reticuloendothelial cells in high yield from a single rat liver by means of Percoll centrifugation and selective adherence. *J. Leukoc. Biol.* **38**, 213–230. https://doi.org/10.1002/jlb.38.2.213 (1985).
47. Mönkemöller, V. *et al.* Primary rat LSECs preserve their characteristic phenotype after cryopreservation. *Sci. Rep.* **8**, 1–10. https://doi.org/10.1038/s41598-018-32103-z (2018).
48. Szafranska, K. *et al.* Quantitative analysis methods for studying fenestrations in liver sinusoidal endothelial cells. A comparative study. *Micron* **150**, 103121. https://doi.org/10.1016/j.micron.2021.103121 (2021).
49. Berg, S. *et al.* Ilastik: Interactive machine learning for (bio)image analysis. *Nat. Methods* **16**, 1226–1232. https://doi.org/10.1038/s41592-019-0582-9 (2019).
50. Mao, H. *et al.* Cost-efficient nanoscopy reveals nanoscale architecture of liver cells and platelets. *Nanophotonics* **8**, 1299–1313. https://doi.org/10.1515/nanoph-2019-0066 (2019).
51. Blomhoff, R., Eskild, W. & Berg, T. Endocytosis of formaldehyde-treated serum albumin via scavenger pathway in liver endothelial cells. *Biochem. J.* **218**, 81–86. https://doi.org/10.1042/bj2180081 (1984).
52. Eskild, W., Kindberg, G. M., Smedsrd, B., Blomhoff, R. & Norum, K. R. Liver endothelial cells after uptake via scavenger receptors. *Biochem. J.* **258**, 511–520 (1989).
53. Schindelin, J. *et al.* Fiji: An open-source platform for biological-image analysis. *Nat. Methods* **9**, 676–682 (2012).
54. Wisse, E., Van Dierendonck, J. H., De Zanger, R. B., Fraser, R. & McCuskey, R. S. On the role of the liver endothelial filter in the transport of particulate fat (chylomicrons and their remnants) to parenchymal cells and the influence of certain hormones on the endothelial fenestrae. *Commun. Liver Cells* **1**, 195–200 (1980).
55. Fraser, R. *et al.* The liver sieve and atherosclerosis. *Pathology* **44**, 181–186. https://doi.org/10.1097/PAT.0b013e328351bcc8 (2012).
56. Fraser, R., Dobbs, B. R. & Rogers, G. W. T. Lipoproteins and the liver sieve: The role of the fenestrated sinusoidal endothelium in lipoprotein metabolism, atherosclerosis, and cirrhosis. *Hepatology* **21**, 863–874. https://doi.org/10.1016/0270-9139(95)90542-1 (1995).
57. Fraser, R. CellsHepaticSinusoid 2.335-338(1989).pdf.
58. de Zanger, R. B. & Wisse, E. The filtration effect of rat fenestrated sinusoidal endothelium on the passage of remnant chylomicrons to the space of Disse. *Sinusoidal Liver Cells* **190**, 371 (1982).
59. Jacobs, F., Gordts, S. C., Muthuramu, I. & De Geest, B. The liver as a target organ for gene therapy: State of the art, challenges, and future perspectives. *Pharmaceuticals* **5**, 1372–1392. https://doi.org/10.3390/ph5121372 (2012).
60. Wright, P. L., Smith, K. F., Day, W. A. & Fraser, R. Small liver fenestrae may explain the susceptibility of rabbits to atherosclerosis. *Arteriosclerosis* **3**, 344 (1983).
61. Fraser, R. *et al.* The opposite effects of nicotine and pantethine on the porosity of the liver sieve and lipoprotein metabolism. *Kupffer Cell Found. Cells Hepatic Sinusoid* **2**, 335 (1989).
62. Szafrańska, K. *et al.* From fixed-dried to wet-fixed to live—Comparative super-resolution microscopy of fenestrations in liver sinusoidal endothelial cells in vitro. *Nanophotonics* **11**, 10 (2022).
63. Simon-Santamaria, J. *et al.* Age-related changes in scavenger receptor-mediated endocytosis in rat liver sinusoidal endothelial cells. *J. Gerontol. A Biol. Sci. Med. Sci.* **65A**, 951–960. https://doi.org/10.1093/gerona/glq108 (2010).
64. Nehlig, A. Interindividual differences in caffeine metabolism and factors driving caffeine consumption. *Pharmacol. Rev.* **70**, 384–411. https://doi.org/10.1124/pr.117.014407 (2018).
65. Bhandari, S. *et al.* Transcriptome and proteome profiling reveal complementary scavenger and immune features of rat liver sinusoidal endothelial cells and liver macrophages. *BMC Mol. Cell Biol.* **21**, 1–25. https://doi.org/10.21203/rs.2.24396/v1 (2020).
66. Van Staveren, W. C. G., Markerink-van Ittersum, M., Steinbusch, H. W. M. & De Vente, J. The effects of phosphodiesterase inhibition on cyclic GMP and cyclic AMP accumulation in the hippocampus of the rat. *Brain Res.* **888**, 275–286. https://doi.org/10.1016/S0006-8993(00)03081-X (2001).
67. Schultz, C., Vaskinn, S., Kildalsen, H. & Sager, G. Cyclic AMP stimulates the cyclic GMP egression pump in human erythrocytes: Effects of probenecid, verapamil, progesterone, theophylline, IBMX, forskolin, and cyclic AMP on cyclic GMP uptake and association to inside-out vesicles. *Biochemistry* **37**, 1161–1166. https://doi.org/10.1021/bi9713409 (1998).
68. Benowitz, N. L., Jacob, P., Mayan, H. & Denaro, C. Sympathomimetic effects of paraxanthine and caffeine in humans. *Clin. Pharmacol. Ther.* **58**, 684–691. https://doi.org/10.1016/0009-9236(95)90025-X (1995).
69. Mandili, G. *et al.* Mouse hepatocytes and LSEC proteome reveal novel mechanisms of ischemia/reperfusion damage and protection by A2aR stimulation. *J. Hepatol.* **62**, 573–580. https://doi.org/10.1016/j.jhep.2014.10.007 (2015).

70. Le Couteur, D. G., Fraser, R., Hilmer, S., Rivory, L. P. & McLean, A. J. The hepatic sinusoid in aging and cirrhosis: Effects on hepatic substrate disposition and drug clearance. *Clin. Pharmacokinet.* **44**, 187–200. https://doi.org/10.2165/00003088-200544020-00004 (2005).
71. Midão, L., Giardini, A., Menditto, E., Kardas, P. & Costa, E. Polypharmacy prevalence among older adults based on the survey of health, ageing and retirement in Europe. *Arch. Gerontol. Geriatr.* **78**, 213–220. https://doi.org/10.1016/j.archger.2018.06.018 (2018).
72. Sano, N. *et al.* New drug delivery system for liver sinusoidal endothelial cells for ischemia-reperfusion injury. *World J. Gastroenterol.* **21**, 12778–12786. https://doi.org/10.3748/wjg.v21.i45.12778 (2015).
73. Hunt, N. J. *et al.* Rapid intestinal uptake and targeted delivery to the liver endothelium using orally administered silver sulfide quantum dots. *ACS Nano* **14**, 1492–1507. https://doi.org/10.1021/acsnano.9b06071 (2020).

Acknowledgements

The authors would like to thank Randi Olsen and Tom-Ivar Eilertsen from Advanced Microscopy Core Facility at UiT for the electron microscopy expertise.

Author contributions

Conceptualization, H.M., K.S., D.W. and P.M.; Data curation, H.M. and K.S.; Formal analysis, H.M., K.S., L.K. and C.H.; Funding acquisition, B.A. and P.M.; Investigation, H.M., K.S. and G.L.; Methodology, H.M., K.S., C.W., R.D., D.L.C. and V.C.; Project administration, P.M.; Resources, C.W., L.C. and P.M.; Software, D.W. and R.D.; Supervision, P.M.; Validation, H.M. and K.S.; Visualization, H.M., K.S. and D.W.; Writing-original draft, H.M. and K.S.; Writing-review & editing, H.M., K.S., L.K., C.H., D.W., B.A., C.W., L.C., G.L., R.D., D.L.C., V.C. and P.M. All authors have read and agreed to the published version of the manuscript.

Funding

Open access funding provided by UiT The Arctic University of Norway (incl University Hospital of North Norway). This study was supported by grants from the Tromsø Research Foundation/Trond Mohn, the University of Tromsø—The Arctic University of Norway, the Research Council of Norway FRIMED grant no. 262538, FRIMED2/FORSKER21 grant no. 325446, Nano2021 grant no. 288565 and Marie Sklodowska-Curie Grant Agreement No. 766181, project: DeLIVER, EU EIC-2021-Pathfinder "DeLIVERY" grant no. 101046928 and the Engelhorn Foundation (Postdoctoral Fellowship to RD).

Competing interests

The authors declare no competing interests.

Additional information

Supplementary Information The online version contains supplementary material available at https://doi.org/10.1038/s41598-023-40227-0.

Correspondence and requests for materials should be addressed to H.M. or K.S.

Reprints and permissions information is available at www.nature.com/reprints.

Publisher's note Springer Nature remains neutral with regard to jurisdictional claims in published maps and institutional affiliations.